Fatty Liver Identification with Novel Anisotropy Features Selected by PSO

Nivedita Neogi
Meghnad Saha Institute of Technology, Kolkata, India
Email: nivedita.neogi@msit.edu.in

Arunabha Adhikari and Madhusudan Roy
West Bengal State University, Barasat, India and Saha Institute of Nuclear Physics, Kolkata, India
Email: arunabha.adhikari@gmail.com, madhusudan.roy@saha.ac.in

***Abstract*—This paper proposes a method to classify ultrasound (US) images of normal and fatty human liver using pattern recognition tools. For classification 32 simple novel features, namely, anisotropy features, proposed by authors, are compared with traditional 200 GLCM features. The extracted features are selected by two methods: i) ranking (Welch's test) and ii) meta heuristic (Particle Swarm Optimisation (PSO)). These selected features are fed into multilayer perceptron (MLP) classifier. It is shown that only 6 anisotropy features, selected by PSO when fed into MLP classifier yield 100% accuracy and the proposed algorithm is much less computational intensive compared to ones found in literature.**

***Index Terms*—anisotropy features, feature selection, particle swarm optimization, fatty liver, ultrasound**

I. Introduction

Pattern recognition comprises essentially three important steps: i) feature extraction, ii) feature selection and iii) classification, although the final step is fully dependent on the first two steps, because the accuracy of any classifier is high for a proper feature set. In pursuit of obtaining more accurate classification, generally more features are added and thus the dimensionality of feature space is increased. The evaluation of the probability distribution is less accurate as the labeled input size remains finite, the performance of classifier may degrade, which is known as curse of dimensionality [1]. Therefore, to produce cost effective pattern recognition with the highest accuracy, optimum feature space is quite important.

In this paper, ultrasonogram (US) of human normal and non-alcoholic fatty (NAFLD) liver images are classified.

Identification of fatty liver or steatosis is important for primary (routine) diagnosis of liver cirrhosis [2] and liver cancer [3]. Worldwide, 6% to 35% (median 20%) of general population is affected by chronic liver disease [4]. Among different imaging modalities US is non-invasive and less expensive and also most reliable for detecting fatty liver [5]. Authors have applied pattern recognition to detect fatty livers from the US images, and a huge number of features are proposed. In many reports, a large number features are extracted and then they are assigned to some ranks following different ranking algorithms. Gradually increasing number of best ranked features is fed to the classifier to achieve optimum classification, Andrade, Silva and Santos [6] classified fatty and normal US liver images by calculating total 325texture features while the best accuracy of 79.77% with 7 features, selected by a stepwise regression method, was achieved by SVM.

Ribeiro, Marinho and Sanches [7] calculated 36 wavelet features for detection of fatty liver images and achieved an overall accuracy of 93.54% using Bayes classifier with 6 features. Singh, Singh and Gupta [8] used 35 texture features out of which 7 best features were selected by linear discriminant analysis, box plot analysis, and Pearson's correlation coefficient. A "Weighted z-score" was proposed as discriminative index in the study and obtained the maximum accuracy of95%. Acharya *et al.* [9] calculated 10,270entropy features from 130 curvelet transform coefficients. Locality Sensitive Discriminant Analysis (LSDA) was used to reduce dimensionality of features and with 6 features, 97.33% accuracy was achieved by PNN. Fatty liver disease was identified by using 128 features. 97.58 % accuracy was achieved using Levenberg-Marquardt Back Propagation network classifier [10]. The total 512 features were extracted from the GIST descriptors and the dimensions of features were reduced by Marginal Fisher Analysis (MFA) and PNN with 17 features which yield 98% accuracy [11]. Acharya et al. [12] calculated 127980 features by Radon Transform (RT) and then Discrete Cosine Transform (DCT) which were reduced by LSDA yielding 30 components and ranked them using minimum redundancy and maximum relevance (mRMR). Fuzzy Sugano (FS) classifiers and Fatty Liver Disease Index (FLDI) gave 100% accuracy with 5 features using 10 fold cross validation method. Feature selection is also tried by meta heuristics. In a different context Acharya *et al*. [13] used RT and bidirectional empirical mode decomposition to extract a total of 264240 features for classification of normal, benign and malignant liver lesions. Particle Swarm Optimization (PSO) was used to select 29 features.

Manuscript received July 3, 2018; revised December 11, 2018.

doi: 10.18178/joig.6.2.160-166

Using these features in PNN classifier 92.95% accuracy was obtained. In summary, as reported in the literature, all authors reduced the feature space and calculated optimized features set for classification using different algorithms to get best results. Although 100% accuracy was already achieved [12] scope of a research for a simpler and less computationally intensive algorithm is still open.

In this work, a meta heuristic algorithm, PSO is used to get optimum feature set for normal and fatty US human liver images.32 novel anisotropy features [14], proposed by the authors, are extracted from each sub-images and PSO is applied for reducing feature space and among 32 features, 6 features are selected by PSO which when fed into classifier and 100% accuracy is achieved. The algorithm is described in Fig. 1.

This paper is organized as follow. Section II describes the details methodology. Section III provides results of this work and section IV concludes the paper.

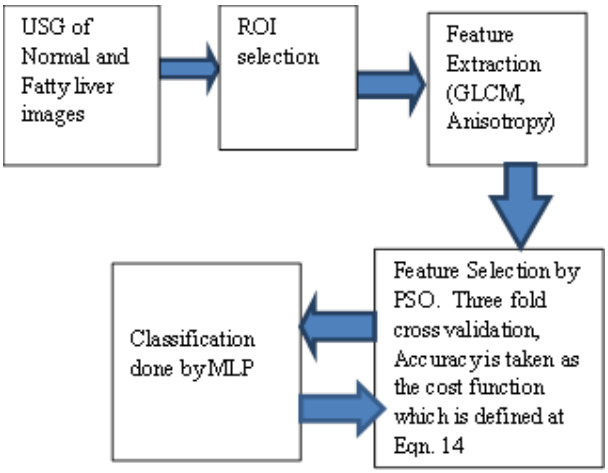

Figure1. Proposed model

II. Methodology

A. Data Collection

Ultrasound images of human livers were collected from Chittaranjan National Cancer Institute, Kolkata. These images are taken with the help of a scanner (Siemens Sonoline Versa Plus) coupled with broad bandwidth phased array convex transducer of probe frequency 3.5 MHz and image field size 6 to 24 cm. All images are labeled as either fatty or normal by a radiologist (pathologically correlated image).

B. Sample Selection

From each US images of human liver of normal and fatty kind sub-images are taken as a sample in this study. Non overlapping small square sub-images represent Regions of Interest (ROI) which are cropped manually from each image.28 normal and 14 fatty US images of human livers are considered for this study. The data set consists of 5 ROIs (Fig. 2a) and from each ultra-sonogram of 28 patients having normal liver, total 140 inputs were made for normal livers. To create same size of fatty liver database to overcome the imbalance data size problem [15] 10 sub-images (Fig. 2b) from each of 14 patients were cropped resulting in a total of 140 inputs for fatty livers.

C. Feature Extraction

Two kinds of features are extracted; they are described in the following section.

1) GLCM texture features

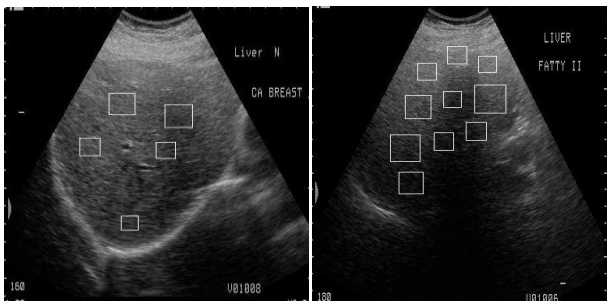

(a) (b)

Figure 2. a: Displaying a typical human normal US liver image with 5 squares with the non-overlapping ROIs: cropped manually from the image avoiding the veins. b: Showing a typical human fatty US liver image with 10 squares with the non- overlapping ROIs: cropped manually from the image avoiding the veins

TABLE I. Descriptors from GLCM Are Explained in above Section. c(I,J) Is GLCM Matrix, mi and mj Are the Mean Values, ΣI and ΣJ Are the Standard Deviations along ith Row and jth Column Respectively

Descriptors	Name	Definition
1	Maximum Probability (Maxp)	$\max_{i,j}(c(i,j))$
2	Angular Second Moment(ASM)	$\sum_i \sum_j c(i,j)^2$
3	Contrast (Const)	$\sum_i \sum_j (i-j)^2 c(i,j)$
4	Inverse element difference moment of order2 (IM2)	$\sum_i \sum_j c(i,j)/(i-j)^2$ $^{i\neq j}$
5	Entropy (Ent)	$-\sum_i \sum_j c(i,j) log_2 c(i,j)$
6	Homogeneity (Homo)	$\sum_i \sum_j c(i,j)/(1+\lvert i-j\rvert)$
7	Correlation (Corr)	$\sum_i \sum_j [(i-\mu_i)(j-\mu_j)c(i,j)] / \sigma_i \sigma_j$
8	Prominence (Prom)	$\sum_i \sum_j (i+j-\mu_i-\mu_j)^4 c(i,j)$
9	Shade(Shade)	$\sum_i \sum_j (i+j-\mu_i-\mu_j)^3 c(i,j)$
10	Inverse difference moment(IDM)	$\sum_i \sum_j c(i,j)/1+(i-j)^2$

GLCM is a most familiar statistical tool for extracting second order texture information from images. Haralick [16] introduced the GLCM features as a measure of texture in the different images which help discriminate the image from each other. Walker, Jackway and Longstaff [17] suggested some more textural features from GLCM. GLCM describes the joint probability that a gray level i occurs at a distance d in direction θ from gray

level j in the texture image and this probability creates the co-occurrence matrix c (i, j | d,θ).In the present study, features are computed from each of the sub-images for different neighborhood pixel pair distances (d = 1, 2, 3, 4 and 8) and directions (θ= 0°, 45°, 90°, 135) and thus, for each sub-image there were 20 GLCM matrices. We have calculated 10 characteristic descriptors from each GLCM matrix yielding a total of 200 features. Descriptors are explained in Table I. Five of them are Haralick's features [16] namely, contrast (Cont), inverse element difference moment of order 2 (Ikmom), angular second moment (Asm), entropy (Ent), correlation (Corr). Shade (shade), prominence (prom), inverse difference moment (Idm) from Walker Jackway and Longstaff. [17] and the remaining two namely, maximum probability (Maxp) suggested by Clausi [18] and homogenity (Homo) described by Tou, Lau and Tay [19] are adopted. 200 features are arranged in such a way so that w^{th} descriptor corresponding to direction θ and pixel pair distance d occupies the position $k = 40(d-1) + \left(\frac{\theta}{45^\circ}\right)10 + w$ in the feature vector. For GLCM, ROIs are re-quantised to 16 grey levels.

2) The proposed anisotropy features

Features pertaining to anisotropy of the image are derived from the following parameters: (i) Edge properties, (ii) GLCM- χ^2, (iii) grey level difference histogram (GLDH) and (iv) pair correlation function (PCF):

Edge properties: Directionality [20] of texture of an image may be estimated from the edges present in the image. The strength and the direction of the edge at any point of the image can be calculated using the following relations:

$$\alpha = \sqrt{\Delta h^2 + \Delta v^2} \text{ and } \theta = \tan^{-1}\left(\frac{\Delta v}{\Delta h}\right) + \frac{\pi}{2} \quad (1)$$

where Δh and Δv are the horizontal and vertical derivatives of the image respectively. From the edge properties we calculate two statistics namely, edge histogram and line-likeness.

Edge Histogram: As the edges in the directions θ and θ+ π are equivalent, all the edges are brought within - π/2 to + π/2 and an histogram of the edge directions is calculated from each sub-image. The edge corresponding to a pixel is counted when its strength α, is above threshold value *T*. It was shown by the authors in their earlier work [14] that the histogram of the edges contains a peak around θ=0 which is attributed to the texture anisotropy.

From Edge Histogram following features are calculated:

FT: formulated by Tamura, Mori and Yamawaki [20] is given below:

$$\text{FT} = 1 - \sum_{\phi}\left(\phi - \phi_p\right)^2 H(\phi) \quad (2)$$

where $H(\phi)$ is the normalized frequency at the angle ϕ and ϕ_p is the angle with maximum frequency. Two other features are proposed for the same purpose by the authors [14].

$$\text{Peakiness} = \max\left(H(\phi)\right) - \overline{H(\phi)}) \quad (3)$$

$$\text{Skewness} = \left(\frac{H(\phi) - \overline{H(\phi)}}{\sigma_{H(\phi)}}\right)^3 \quad (4)$$

Line-Likeness: Line-Likeness is another feature proposed by Tamura, Mori and Yamawaki [20]. The original values of θ as calculated from eq. (1) are rounded off to the nearest multiple of π/4 and the multiplier is called the edge code. A edge code co-occurrence matrix P_{ed} is calculated, the (i,j)th element of which is the frequency of the pixel pairs with edge code i and j separated by one pixel along the direction indicated by i. Line –likeness is calculated from P_{ed} by the following formula:

$$\text{Llike} = \sum_{i=1}^{4}\sum_{j=1}^{4} P_{ed}(ij)\cos\left|(i-j)\frac{2\pi}{4}\right| / \sum_{i}^{4}\sum_{j}^{4} P_{ed}(ij) \quad (5)$$

GLCM-χ^2: The randomness of the image texture may be quantified by a statistical score following a method initially proposed by Zucker and Terzopoulos [21]. If the texture has uniformity only in a particular θ and d then GLCM with the appropriate values of d and θ would be more diagonal while other choices would lead to more randomness. If there is any regularity, intensity value of the first pixel should influence the probabilities of observing different intensity values of the second pixel and consequently, the columns of GLCM are correlated. In the absence of such bias, (i,j)th element of GLCM which is the joint probability may be written as $p_{ij} = r_i c_j$ where $r_i = \sum_{j=1}^{m} p_{ij}$ = (the probability that the first pixel is *i)* and $c_j = \sum_{i=1}^{m} p_{ij}$ = the probability that the second pixel is *j* (here *m* is the number of quantization levels). A chi-square parameter is designed under the null hypothesis that the intensity values of the pixel pairs are independent by the following formula:

$$\chi^2 = \sum_{i=1}^{m}\sum_{i=1}^{m} \frac{(p_{ij} - r_i c_j)^2}{r_i c_j} \quad (6)$$

Thus with larger value of χ^2 the randomness is less. An image comprising directed line segments would show the largest value of χ^2 in that direction and scale. We proposed that the value of χ^2 can be taken as an indicator to measure the information content of a given GLCM and use this score to compare the 20 GLCMs and showed that [14] at d=1, θ=0. χ^2 values are much higher than the other combinations signifying that the inherent pattern in the texture is more pronounced in this scale and orientation.

GLDH: GLDH [22] is a vector whose *i*th element represents the probability that the absolute value of the difference of grey levels between two pixels separated by a given distance along a particular direction is *i.* Two parameters namely, mean and variances of grey level difference are calculated from the GLDH vector. Average values of these parameters over all sub-images for 20 combinations of d, θ are calculated and found that the average value is minimum at (d, θ) = (1, 0) and so it suggests that texture regularity is the most prominent in this scale and orientation [14].

PCF: PCF [23] is calculated based on the following formula and the average values are taken over all pixels $\vec{x}$ in the sub-image:

$$g(\vec{r}) = \frac{\overline{(I(\vec{x})-\mu)(I(\vec{x}+\vec{r})-\mu)}}{(I(\vec{x})-\mu)^2} \quad (7)$$

$g(\vec{r})$-averaged over all sub-images and has a maximum at (d, θ) = (1, 0) as shown in our previous work [14].

Features derived from above parameters: Each of the above parameters (mentioned in above) is shown to have noticeable asymmetry in their distribution at different distances and orientations. This may be explicitly exploited in designing two types of features namely, scale-angle and anisotropy index:

$$\text{Scale-angle} = f(1,0) - \langle f(d,\theta)\rangle_{d,\theta} \quad (8)$$

where f is parameter of interest f (1, 0) denotes its value at (d, θ)=(1, 0) and the average in the last term is taken over all d and θ's.

$$\text{Anisotropy - index} = \langle\langle f(d,0) - f(d,\theta)\rangle_\theta\rangle_d \quad (9)$$

The scale-angle feature denotes how the value of the parameter at (d, θ) = (1, 0) is different from its average taken over all distances and directions and the anisotropy index measures the average deviation of the parameter at 0^o from its average over all directions. These two features are calculated from each sub-image belonging to normal and fatty classes for GLDH-mean, GLDH- variance, PCF and GLCM-χ^2. Moreover, PCF at different values of d, θ are also treated as features. These features along with 4 Edge Property features amount to total 32 anisotropy features and are summarized in Table II.

TABLE II. THE NAME OF THE 32 ANISOTROPY FEATURES WHICH ARE DESCRIBED IN ABOVE SECTION

Feature number	Name of the anisotropy features
1.	Peakiness
2.	Skewness
3.	FT
4.	Anisotropy index (GLCM- χ2)
5.	Scale-angle index (GLCM- χ2)
6-25.	PCF (20 different d and θ)
26.	Scale-angle index (PCF)
27.	Anisotropy index (PCF)
28.	Scale-angle index (GLDH mean)
29.	Anisotropy index (GLDH mean)
30.	Scale-angle index (GLDH variance)
31.	Anisotropy index (GLDH variance)
32.	Llike

D. Feature Selection

1) Ranking method

200 GLCM features and 32 anisotropy features' effectiveness are measured by well- known Welch's test [24]. The ability of a feature to distinguish between the sub-images of the normal livers and those from the fatty liver is explored. Note that any assumption about the equality of variance of the features in the two classes is not made and hence instead of student's t, Welch's t statistic, as described in (10) and (11),

$$t = \sqrt{n}\frac{x_1 - x_2}{\sqrt{s_1^2 + s_2^2}} \quad (10)$$

is computed for each feature. n is the number of sub-images in each of the classes, x_1 and x_2 are the means of the relevant feature in normal and fatty class, s_1 and s_2 the respective standard deviations. The degree of freedom is calculated by the formula,

$$\text{d} = (n-1)\frac{\left(s_1^2 + s_2^2\right)^2}{s_1^4 + s_2^4} \quad (11)$$

The p values corresponding to each t and d are obtained from Student's t distribution. p denotes the probability that the two mean values are statistically the same. Hence, less the p value higher the probability that the values of the feature in the two relevant classes are statistically different. A feature with a low p value therefore is a potentially good feature for classification.

2) PSO

PSO [25] a population based meta heuristic optimization technique which is inspired by social behavior of bird flocking or fish schooling.

PSO is an optimization algorithm in a multivariable space. A population of particles is modeled to move in an n-dimensional space S in search of the position vector $\vec{x}$ that maximizes a fitness function $f(\vec{x})$. All particles have velocities which impart inertia to the particles.

Initial positions of the particles are randomly assigned and subsequently updated. In every iteration, each particle is moved by following two best values. The first one is the best position (as per fitness) a particular particle has achieved so far. This value is called personal best or $\overrightarrow{pbest}$. Another best value that is the one obtained so far by some particle in the population. This best value is a global best and called $\overrightarrow{gbest}$. After finding the two best values, the particle updates its velocity $v(t)$ and position $x(t)$ with following equation (12) and (13).

$$\vec{v}(t+1) = \vec{v}(t) + c_1 r_1\left(\overrightarrow{pbest}(t) - \vec{x}(t)\right) + c_2 r_2(\overrightarrow{gbest}(t) - \vec{x}(t)) \quad (12)$$

$$\vec{x}(t+1) = \vec{x}(t) + \vec{v}(t+1) \quad (13)$$

r_1 and r_2 are random numbers between (0,1). c1, c2 are learning factors and the value of c1 and c2 is 1.4962 as suggested by authors [26].

In the present work, PSO is used to select NF number of features out of a set of n features. For GLCM features n=200 and for anisotropy features n=32. Number of particle for the present work is taken as 10. Algorithm of implementation of PSO for feature selection follows:

NF=number of feature to be selected
Initialize position vector of each particle randomly in a n-dimensional space
Set initial velocity =0 for each particle
DO
FOR each particle
    Find the highest NF components of the n-dimensional position vector
    Select the corresponding features in the n dimensional feature vectors
Run MLP with selected NF features

Calculate average of accuracy in three fold cross validation as the fitness function corresponding to the current position
Update the pbest
END
Update the gbest
FOR each particle
Update the velocity and the position by PSO update rule (12) and (13)
END
WHILE maximum iterations or minimum error criteria is not attained

E. Classifier

Levenberg- Marquardt back propagation neural network

To classify the normal and fatty liver images a supervised neural network classification method, Levenberg-Marquardt back propagation algorithm [27] is used to train the system. The network comprises three layers of which the input layer contains the number of features and output layer contains 1 neuron. The output neuron value is a real number belonging to the interval [0, 1]. The target for normal and fatty class is set as 0 and 1. The predicted class is identified as normal when output <0.5 and as fatty in the other case. For all subsequent analyses in this study, the number of neurons at hidden layer is fixed at 10.

F. Assessment of Classification

Accuracy

Accuracy is the measurement of correctness. Accuracy is calculated as

$$\text{Accuracy} = \frac{N_c}{N_T} * 100 \quad (14)$$

where N_c is the correctly classified sub-images, $N_T$is the total number of sub-images. All results are reported with three fold cross validations.

III. Result

In this study, the proposed method is developed by MATLAB 2016 environment in a standalone personal computer using Intel i7 3770 processor @3.40 GHz with 16 GB RAM and 64 bit Windows 7 operating system.

The data base consist 140 samples of normal and 140 samples of fatty sub-images. From each sub-images the following feature sets are obtained.

Feature set 1: GLCM feature: 200 GLCM features as described in Table I.

Feature set 2: Anisotropy feature: 32 anisotropy features as described in Table II.

From the extracted features, best features are selected by two methods: i) ranking (Welch's test) and ii) meta heuristic method (PSO).

Best 20 GLCM and 20 anisotropy features are taken according to p-value (<.0001) by ranking method and are used to train MLP. The performance of best 20 GLCM feature and best 20 anisotropy features by ranking is shown in Table III.

The performance of selected features by PSO with progressively increasing number of anisotropy features is shown in Table IV.

Since PSO selects the optimum feature set, the accuracy with 2 features is better than the best 20 ranked features. 100% accuracy is achieved with 6 features and the result could be maintained even with 20 features (refer to Fig. 3). Furthermore, the change in the number of features in the range 6 to 20 does not alter the accuracy but the PSO converges faster. Similar exercise of selection of GLCM features by PSO reveals that with 6 features the accuracy is 69.6%. The best accuracy is found for 10 features i.e. 70.9% (shown in Table V). However, the increase in the number of features up to 20 does not show much change in accuracy but again PSO convergence faster. Evidently PSO selected features are much better than the best 20 GLCM features found by ranking.

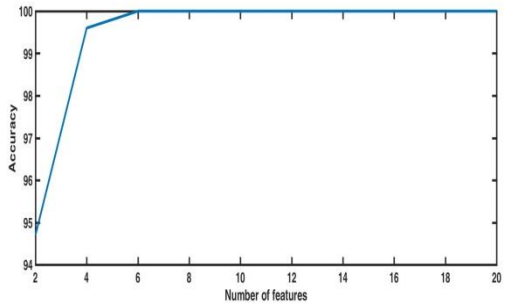

Figure 3. Figure shows that 100% accuracy is achieved with 6 features selected by PSO and the result could be maintained even with 20 features

When PSO is used to select 6 to 20 numbers of features, 100% accuracy is achieved in each case. However, when PSO selects set of (NF + 1) features, the set does not turn out to be a simple extension of the set of NF features selected by PSO. Precisely, the sets with varying number of features appear to be independent. Scale-angle index of PCF (feature no 26) is the most common feature that appears in all these sets. Interestingly, this feature does not belong to the best 20 features ranked by Welch's test.

IV. Conclusion

The proposed algorithm classifies US images of normal and fatty human liver using pattern recognition tool. From each class 140 samples are taken for this study. 32 proposed anisotropy features as well as 200 traditional GLCM features are extracted from these samples. The various authors as found in the literature used different ranking methods for feature selection. In this study Welch's test, a ranking algorithm is used for feature selection. Another algorithm PSO is applied for searching feature space for the optimum set. From the output based on these two feature selection criteria, it is observed that the feature selection by PSO is much superior to the feature selection by ranking method. 100% accuracy is achieved using 6 proposed anisotropy features. However, with increase in the number of features to be selected by

PSO, the search becomes faster. Comparing Table III and Table IV it is evident that PSO selects more efficient features in terms of accuracy. Among 32 anisotropy features Scale-angle index of PCF (feature no. 26) is the most stable features because it appears in all feature sets excluding when number of features is 2 (refer to Table III). This feature measures the difference of correlation between two pixel intensities separated horizontally by 1 pixel and the correlation when the pixels are separated in any other manner. The mean value of this feature is higher in case of fatty images indicating that the anisotropy effect is much stronger in case of fatty images. Trend of the day is classification done by deep learning which involves huge memory and computation time and large database. Our proposed method, on the other hand, will be applicable when these resources are inadequate. Although 100% accuracy using FS classifier and FLDI was achieved by others [12], their methods need several steps of pre-processing and extraction of 127980 primary features before arriving at the reduced features but our proposed method has no pre-processing and would call for extraction of only 6 selected anisotropy features. The novelty of this work originates from the efficiency of anisotropy features.

TABLE III. SHOWS THE BEST 20 GLCM (SET 1) AND ANISOTROPY (SET 2) FEATURES RANKED BY WELCH'S TEST. NF DENOTES NUMBER OF FEATURES, ACC DENOTES ACCURACY WHEN MLP IS RUN WITH SET 1 AND SET 2.

Feature set	NF	Acc	Feature set denoted by feature number																			
Set 1	20	57%	1	2	3	4	5	6	8	42	43	44	45	46	48	83	84	85	86	88	126	176
Set 2	20	93%	1	2	4	5	6	7	8	10	12	14	16	17	18	20	21	24	25	27	28	30

TABLE IV. RESULT SHOWS ANISOTROPY FEATURE SETS SELECTED BY PSO. NF DENOTES NUMBER OF FEATURES, ACC DENOTES ACCURACY AND ITR DENOTES THE NUMBER OF ITERATION OF PSO

NF	Acc	Itr	Feature set denoted by feature number																			
2	94.7%	42	3	22																		
4	99.6%	10	1	26	27	20																
6	100%	25	6	14	8	29	26	24														
8	100%	11	26	12	20	5	7	13	11	4												
10	100%	4	4	19	13	5	7	26	23	6	31	1										
12	100%	2	7	1	25	26	3	13	8	31	16	6	14	11								
14	100%	4	32	17	19	9	29	12	18	24	15	22	21	8	6	26						
16	100%	3	10	24	18	6	1	29	9	31	3	26	4	7	15	2	17	13				
18	100%	1	6	30	18	19	28	22	23	10	24	21	11	20	26	16	9	32	1	8		
20	100%	1	13	29	16	7	18	2	26	20	17	24	15	5	8	25	9	31	27	12	10	6

TABLE V. RESULT SHOWS THE NATURE OF CHANGE OF GLCM FEATURE SETS SELECTED BY PSO. NF DENOTES NUMBER OF FEATURES, ACC DENOTES ACCURACY AND ITR DENOTES THE NUMBER OF ITERATION OF PSO.

NF	Acc	Itr	Feature set denoted by feature number																			
6	69.6%	93	20	13	60	39	35	129														
10	70.9%	47	4	67	9	106	175	100	28	49	125	104										
15	69.2%	88	45	136	173	72	141	123	139	7	126	156	12	79	143	21	172					
20	68.9%	44	86	99	156	186	41	199	4	84	173	28	195	95	196	147	176	27	166	133	121	170

ACKNOWLEDGEMENT

We would like to thank Dr. Suparna Majumdar, Department of Radio diagnosis, Chittaranjan National Cancer Institute, Kolkata-700026, India, for providing the USG of livers for this study.

REFERENCES

[1] R. E. Bellman, *Adaptive Control Processes: A Guided Tour*, Princeton University press, 2015, p. 94.
[2] J. M. Clark and A. M. Diehl, "Nonalcoholic fatty liver disease: An under recognised cause of cryptogenic cirrhosis," *JAMA*, vol. 289, pp. 3000-3004, 2003.
[3] M. S. Ascha, I. A. Hanounch, R. Lopez, T. A. R Tamini, A. F. Feldstein, and N. N. Zein, "The incidence and risk factors of hepatocellular carcinoma in patients with non-alcoholic steatohepatitis," *Hepatology*, vol. 51, pp. 1972-1978, 2010.
[4] S. G. Sheth and S. Chopra, "Epidemiology, clinical features and diagnosis of nonalcoholic fatty liver disease in adults," *Waltham (MA): UpToDate*, 2017.
[5] A. Duseja, "Nonalcoholic fatty liver disease in India–a lot done yet more required!" *Indian J. of Gastroenterology*, vol. 29, no. 6, pp. 217-225, 2010.
[6] A. Andrade, J. S. Silva, J. Santos, and P. Belo-Soares, "Classifier approaches for liver steatosis using ultrasound images," *Procedia Technology*, vol. 5, pp. 763-770, 2012.
[7] R. Ribeiro, R. T. Marinhoand, and J. M. Sanches, "Global and local detection of liver steatosis from ultrasound," in *Proc. IEEE Annual International Conf. in Engineering in Medicine and Biology Society*, 2012, pp. 6547-6550.
[8] M. Singh, S. Singh, and S. Gupta, "An information fusion based method for liver classification using texture analysis of ultrasound images," *Inf. Fusion*, vol. 19, pp. 91-96, 2014.
[9] U. R. Acharya, *et al.*, "Automated characterization of fatty liver disease and cirrhosis using curvelet transform and entropy features extracted from ultrasound images," *Computers in Biology and Medicine*, vol. 79, pp. 250-258, 2016.
[10] L. Saba, *et al.*, "Automated stratification of liver disease in ultrasound, an online accurate feature classification paradigm," *Computer Methods and Programs in Biomedicine*, vol. 130, pp. 118-34, 2016.
[11] U. R. Acharya, *et al.*, "Decision support system for fatty liver disease using GIST descriptors extracted from ultrasound images," *Inf. Fusion*, vol. 29, pp. 32-39, 2016.
[12] U. R. Acharya, *et al.*, "An integrated index for identification of fatty liver disease using radon transform and discrete cosine transform features in ultrasound images," *Inf. Fusion*, vol. 31, pp. 43-53, 2016.

[13] U. R. Acharya, *et al.*, "Automated diagnosis of focal liver lesions using bidirectional empirical mode decomposition features," *Computers in Biology and Medicine*, 2018.
[14] N. Neogi, A. Adhikariand, and M. Roy, "Anisotropy of the texture in the ultra-sonogram of human livers," in *Proc. IEEE International Conference on Information Science*, August 2016, pp. 114-119.
[15] N. V. Chawla, K. W. Bowyer, L. O. Hall, and W. P. Kegelmeyer, "SMOTE, synthetic minority over-sampling technique," *J. Artificial Intelligence Research*, vol. 16, pp. 321-357, 2002.
[16] R. M. Haralick and K. Shanmugam, "Textural features for image classification," *IEEE Trans. on Systems Man and Cybernetics*, vol. 3, no. 6, pp. 610-621, 1973.
[17] R. F. Walker, P. Jackway and I. D. Longstaff, "Improving co-occurrence matrix feature discrimination," in *Proc. 3rd Conf. on Digital Image Computing, Techniques and Application*, 1995, pp. 643-648.
[18] D. A Clausi, *Texture Segmentation of SAR Sea Ice Imagery*, Waterloo, Ontario, Canada N2L 3G1: University of Waterloo, 1996.
[19] J. Y. Tou, P. Y. Lau, and Y. H. Tay, "Computer vision-based wood recognition system," in *Proc. International Workshop on Advanced Image Technology*, 2007.
[20] H. Tamura, S. Mori, and T. Yamawaki, "Textural features corresponding to visual perception," *IEEE Trans. on Systems Man and Cybernetics*, vol. 8, no. 6, pp. 460-473, 1978.
[21] S. W. Zuckerand and D. Terzopoulos, "Finding structure in co-occurrence matrices for texture analysis," *Computer Graphics and Image Processing*, vol. 12, no. 3, pp. 286-308, 1980.
[22] D. Chetverikov, "GLDH based analysis of texture anisotropy and symmetry, an experimental study," in *Proc. IEEE 12th IAPR International Conference on Computer Vision & Image Processing*, 1994, vol. 1, pp. 444-448.
[23] R. Lehoucq, *et al.*, "Analysis of image vs position scale and direction reveals pattern texture anisotropy," *Frontiers in Physics*, vol. 2, p. 84, 2015.
[24] B. L. Welch, "The generalization of student's' problem when several different population variances are involved," *Biometrika*, vol. 34, no. 1/2, pp. 28-35, 1947.
[25] J. Kennedy and R. Eberhart, "Particle swarm optimization," in *Proc. IEEE Conf. Neural Networks*, 1995, pp. 1942-1948.
[26] Machine Learning. [Online]. Available: http://yarpiz.com/category/machine-learning
[27] D. E, Rumelhart, G. E. Hinton, and R. J. Williams, "Learning representations by back-propagating errors," *Nature*, vol. 323, no. 6088, pp. 533-536, 1986.

Nivedita Neogi received M.E. degree in Information Technology from West Bengal University of Technology, West Bengal, India in 2007. She is persuing the Ph.D. degree in Computer Science from West Bengal State University, West Bengal, India. Now she is Assistant Professor in the department of Information Technology at Meghnad Saha Institute of Technology (Techno India Group), Kolkata, India. Her research interest area is image processing, texture analysis and pattern recognition.

Arunabha Adhikari, Ph.D., obtained his masters in Physics from Calcutta University in Physics. He worked in Saha Institute of Nuclear Physics as a senior research fellow and obtained doctoral degree from Calcutta University. His initial research was in Biophysics. Topic of his Ph.D. research was related to theoretical simulation of Calcium Action Potential. Later we worked in the laboratories of electrophysiology in Indian Institute of Science, Bangalore, India and Department of Physiology, University of Saarland, Germany. He has been teaching physics for the last 20 years and presently working in the West Bengal State University. His present interests concern computational physics, computational neuroscience and application of neural network in biomedical image processing.

Madhusudan Roy, Ph.D. obtained his masters in Physics and Ph. D. degree from the North Bengal University in 1983 and 1989 respectively. He has been working in the fields of material science, gas sensors, photoacoustic imaging, and image analysis. Presently, he is working in Saha Institute of Nuclear Physics, Kolkata, India.